IOSR Journal of Applied Chemistry (IOSR-JAC)
e-ISSN: 2278-5736.Volume 16, Issue 2 Ser. I (February 2023), PP 64-77
www.iosrjournals.org

DNA Interactions, Biological activities of Co(II), Ni(II), Cu(II) Complexes of 2-methoxy 5-trifluoromethyl benzenamine Schiff base: Synthesis, Characterization

Swathi M, Shivaraj*
Department of Chemistry, Osmania University, Hyderabad, Telangana-500007, India

Abstract:
Novel Schiff base ***((E)-(5-trifuoromethyl)-2-methoxyphenylamino)methyl)-4-bromophenol*** *and its binary Co(II), Ni(II), Cu(II) complexes were synthesized. The structures of all the compounds have been characterized on the basis of elemental analysis, FT-IR, NMR, UV-Visible, ESI -Mass, TGA, ESR, and magnetic moments. Based on the analytical and spectral data a square planar geometry has been assigned to Ni (II), Cu (II) complexes and octahedral geometry has been assigned to Co (II), in which the Schiff base act as bidentate ligand, coordinating through the azomethine nitrogen and phenolic oxygen atom. Geometry optimized structures have also been illustrated using Chem 3D software. DNA binding ability of these complexes was studied on CT-DNA by using UV-Vis absorption, fluorescence. DNA cleavage ability of the complexes was examined on pBR322 DNA by using gel electrophoresis method. All the DNA binding studies reveal that they are good intercalators. The bioefficacy of the ligand and its complexes were examined against the growth of bacteria and fungi in vitro to evaluate their antimicrobial potential. The screening data revealed that the complexes showed more antimicrobial activity than the corresponding free ligand. Antidiabetic, antioxidant, anti-cancer activity (against KB3, MCF7 cell lines) have also been performed and resulted that copper complex exhibited higher activity than other complexes and its ligand.*
Key words: *Schiff Base, Metal complexes, Biological activity.*

Date of Submission: 14-02-2023 Date of Acceptance: 28-02-2023

I. Introduction

DNA is the principal intracellular target of anticancer medicines due to its key function in replication and transcription. Intercalation is one of the cancer-fighting medications' modes of action. A promising family of anticancer medicines that fulfill this goal are metallo intercalators, which contain planar aromatic rings and can undergo non-covalent interactions with DNA molecules via pi-pi stacking and dipole-dipole interactions [1]. Intercalation is an efficient binding mechanism that can trigger cellular breakdown [2]. Schiff base compounds are an important class of ligands whose rich coordination chemistry has attracted much research [3]. They have numerous applications in various fields. These compounds have been utilized in numerous biological applications over the years, including anticancer and antimalarial therapy etc., [4]. Schiff bases can establish coordination bonds with numerous transition metal ions via phenolic or azomethine groups; as a result, they have been utilized for the metal complexes synthesis [5, 6] due to their facile creation and strong metal binding capacity. Transition metal (II) complexes with aromatic Schiff bases have been intensively researched due to their strong interaction with DNA through intercalation or surface interactions and their potential DNA cleavage activities [7]. Numerous inorganic chemists have been attracted to the medical applications of Cu, Ni, and Co cationic complexes [8] because of the bio essential, enzymatic activity, and oxidative nature of transition elements, which are vital to humans. In recent studies, metal complexes capable of cleaving DNA under physiological settings have garnered significant interest not only for their prospective uses in artificial nucleic acid chemistry, but also for their intriguing role as anticancer agents [9, 10]. The synthesis, characterization, biological activity, anti oxidant activity and DNA binding with M (II) complexes of various Schiff bases have been reported earlier from our laboratory [11-15]. In light of the aforementioned, this article describes the synthesis, structural characterization, DNA interaction, and biological research of Cu(II), Ni(II), and Co(II) complexes with 2-methoxy-5-trifluoromethyl benzenamine Schiff base.

II. Experimental

Materials and instrumentation

Sigma-Aldrich, Hi-Media Ltd, Merck, and Finar provided the reagents and solvents used in this study. Standard procedures were used to prepare distilled and double distilled water for use in binding and cleavage experiments. Genie Bangalore, India provided the CT-DNA and per 322 DNA. A Polson device was used to determine the melting points (Model No. MP-96). For ^{1}H and ^{13}C structural investigation, NMR spectra were viewed (in ppm) using a Bruker AV-400 spectrometer with a range of 400 and 100 MHz, respectively. The FTIR spectra were recorded on a Shimadzu IR Prestige-21 spectrophotometer using KBr pellets in the region of 4000-250 cm^{-1}. Shimadzu UV-Vis 2600 spectrophotometer provided electronic spectral data. Micro analytical procedures on a Perkin Elmer 240C (USA) elemental analyzer were used to measure the percentage composition of C, H, N, and S. On a VG AUTOSPEC mass spectrometer, ESI mass spectrometry was performed. The JES-FA200 ESR spectrometer was used to record ESR spectra at -196 ° C. (JEOL-Japan. On a JASCO spectrofluorometer FP-8500, a fluorescence quenching investigation was carried out. Thermo grams of the complexes were carried on Mettler Toledo Star system in the temperature range of 27–1000°C. Melting points of the Schiff bases and their M(II) complexes were determined on Polmon instrument (Model no. MP-96). . The thermo gravimetric analysis was carried out in a dynamic nitrogen atmosphere with a heating rate of 10 °C min^{-1} using a Shimadzu TGA-50H in the temperature range of 27–1000 °C**.** All the experimental techniques for DNA interaction studies, cleavage studies, and biological assays are briefly mentioned in the supplementary file no.1.

Synthesis of Schiff base ligand : HL^1

Magnetically stirring a hot methanolic solution of 2-methoxy-5-trifluoromethylbenzenamine (10 mmol) and 5-bromo salicylaldehyde (10 mmol) for six hours at 60–80 °C. TLC was used to monitor the progress of the reaction and the purity of the product. The reaction produces a brown-colored precipitate, which was filtered and dried. The **scheme I** depicts the synthetic route for Schiff base and their complexes.

Characterization of Schiff base ligand : HL^1

HL^1: ((E)-(5-trifuoromethyl)-2-methoxyphenylamino)methyl)-4-bromophenol

Color: Reddish brown, Yield: 90%; M.pt: 99 ^{o}C. Anal. Calc**.** (found) C, 48.15 (47.80); H, 2.96 (2.91); Br, 21.36 (20.15); F, 15.23 (14.80); N, 3.74 (3.69); ^{1}H NMR (400 MHz, $CDCl_3$): δ 13.44 (s, 1H), 8.65 (s, 1H), 7.06 (s, 1H), 7.26 (d, *J*=6.2, 2H), 7.54 (d, *J*= 2.2 Hz, 2H), 6.9 (s, 1H), 3.95 (s, 3H) **(Figure S1**). ^{13}C NMR (100 MHz, $CDCl_3$): δ 162.52, 160.49, 154.48, 139.57, 136.72, 135.79, 133.83, 132.41, 126.62, 125.48, 120.58, 119.15, 116.50, 112.01, 110.27, 56.30. **(Figure S2)** IR (KBr) (cm^{-1}): $\nu_{(OH)}$ 3453, $\nu_{(HC=N)}$ 1622, $\nu_{(C-O)}$ 1130, UV (DMSO) λ_{max}/nm (cm^{-1}): 257 (38910), 357 (28011), **(Figure S9);** MS (ESI): m/z 373 $[M-2]^{-}$ **(Figure S4)**

Synthesis of binary Metal(II) complexes:-(A-C)

Refluxing hot methanolic solutions (10 mL) of each metal acetate (0.5 mmol) $[Cu(CH_3COO)_2.H_2O]$ / $[Co(CH_3COO)_2.4H_2O]$ / $[Ni(CH_3COO)_2.2H_2O]$ and schiff base in 1:2 ratio that yields $[Cu(HL^1)_2]$ / $[Co(HL^1)_2.2H_2O]$ / $[Ni(HL^1)_2]$. TLC was used to monitor the course of the reaction and the purity of the product for six hours at 60–80 °C and 1 mmol of Schiff base. By filtration and drying, coloured precipitates were collected. The **scheme I** depicts the synthetic route for Schiff base.

Characterization of binary metal(II) complexes:-(A-C)

(A): $[Co(HL^1)_2(H_2O)_2]$

Color: Pale Brown, Yield: 83%, M.pt: ~90^{o}C, Anal. Calc. (Found) C, 42.83 (42.78); H, 2.88 (2.75); Br, 19.00 (18.96); F, 13.55 (13.19); N, 3.33 (3.28); Co,7.01 (6.93); IR (KBr) (cm^{-1}): $\nu_{(O-H)}$ 3426 $\nu_{(HC=N)}$ 1593, $\nu_{(C-O)}$ 1122, $\nu_{(M-O)}$ 530, $\nu_{(M-N)}$ 436;UV-Vis (DMSO) λ_{max}/nm (cm^{-1}): 260 (38461), 351 (28490), 439 (22779), 555 (18018), 565 (17699); μ_{eff} (BM): 4.22;MS (ESI): m/z 841 $[M]^{+}$ **(Figure S5)**. The **scheme I** depicts the synthetic route for Schiff base and its complexes.

(B):$[Ni(HL^1)_2]$:

Color: Pale yellow, Yield: 72%, M.pt: 310^{o}C, Anal. Calc. (Found) C, 44.76 (44.55); H, 2.50 (2.46);Br, 19.85 (19.74); Ni, 7.29 (7.04); F, 14.16 (14.10); N, 3.48 (3.45); IR (KBr) (cm^{-1}): $\nu_{(HC=N)}$ 1609, $\nu_{(C-O)}$ 1125, $\nu_{(M-O)}$ 511, $\nu_{(M-N)}$ 436; UV-Vis (DMSO) λ_{max}/nm (cm^{-1}): 258 (38759), 425 (23529), 545 (18348); μ_{eff} (BM): 0; MS (ESI): m/z 804 $[M+2]^{+}$ **(Figure S6)**

(C):$[Cu(HL^1)_2]$:

Color: Black, Yield: 72%, M.pt: 320^{o}C, Anal. Calc. (Found) C, 44.49 (44.15); H, 2.49 (2.46);Br, 19.73 (19.34); Cu, 7.85 (7.34); F, 14.08 (14.01); N, 3.46 (3.35); IR (KBr) (cm^{-1}): $\nu_{(HC=N)}$ 1599, $\nu_{(C-O)}$ 1128, $\nu_{(M-O)}$ 517, $\nu_{(M-N)}$

465; UV-Vis (DMSO) λ_{max}/nm (cm^{-1}): 259 (38610), 287 (34843), 415 (24096), 548 (18248); μ_{eff} (BM): 1.86; ESR: $g_{\parallel}$= 2.1881, $g_{\perp}$=2.1295, G=1.460, $A_{\parallel}$ =0.0167 cm^{-1}, $g_{\parallel}/A_{\parallel}$ =131 cm; MS (ESI): m/z 810, $[M]^+$, $[M+2]^+$ **(Figure S7)**

Reaction Scheme:

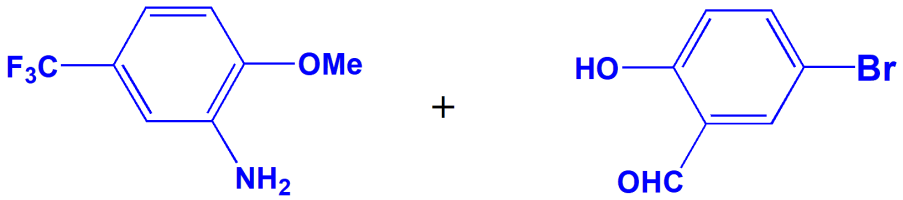

2- methoxy 5-trifluoro methyl benzenamine

5-bromo salicylaldehyde

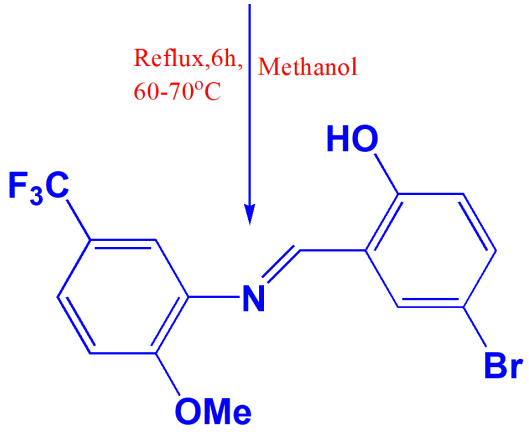

2-((*E*)-(5-(trifluoromethyl)-2-methoxyphenylimino)methyl)-4-bromophenol

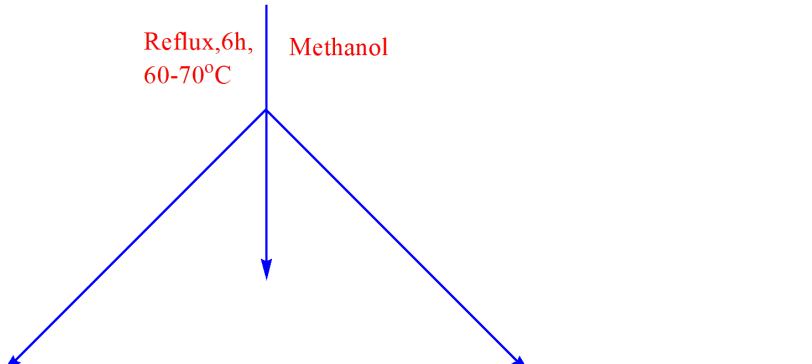

A $(C_{30}H_{24}Br_2CoF_6N_2O_6)$ **B** $(C_{30}H_{20}Br_2F_6N_2NiO_4)$ **C** $(C_{30}H_{20}Br_2CuF_6N_2O_4)$

Scheme 1: Reaction Scheme for the synthesis of Schiff base ligand (HL^1) and its respective metal complexes

III. Results and Discussions

Characterization of ligand: **HL^1**

The synthesized ligand (**HL^1**) is brown in color, non-hygroscopic, thermally stable at room temperature, and completely soluble in Methanol, Chloroform, Dimethylfluoride, and Dimethyl sulfoxide, but insoluble in water. The purity of the ligand was checked by TLC method. It is characterized by elemental analysis and various spectral techniques (NMR, FT-IR, UV, ESI-MASS) (NMR, FT-IR, UV, ESI-MASS). Based on the analytical data the formulae of the ligand is (**$C_{15}H_{11}BrF_3NO_2$**)**- HL^1**

Characterization of complexes

All the synthesized complexes (A-C) are colored solids, non-hygroscopic, thermally stable at room temperature, and completely soluble in methanol, chloroform, dimethylfluoride, and dimethyl sulfoxide, but insoluble in water. The purity of the complexes was examined using TLC. The elemental analysis and spectral methods (NMR, FT-IR, ESR, TGA, ESI-MASS etc) have been employed for the characterization of these complexes. Using analytical data, the M:L ratio is found to be 1:2. For all the complexes the molar conductance values were found to be within the range of 4-5 Ω^{-1} cm^2 mol^{-1}, suggesting that they are non-electrolytic.

Spectral Characteristics

FTIR Spectra

The IR spectra of the synthesized compounds were recorded in order to know the coordination of the ligand with the metal ions . FTIR spectra were recorded on a Shimadzu IR Prestige-21 spectrophotometer using KBr pellets in the region of 4000-250 cm^-. Complexes are confirmed by the emergence of a distinctive bands for the azomethine group (N = CH-) at around 1593 to1609 cm^{-1}, $\upsilon_{(C-O)}$ bands at (1122 to 1128 cm^{-1}) observed slight lower regions with respect to ligand bands and disppearance of the υ(OH) band also confirms complexation. Additionally, in the case of cobalt complex **A**, bands were observed in the region 750-850 cm^{-1} and at 3426 cm^{-1} suggesting the presence of coordinated water [16]. Apart from these bands the M-N and M-O bands also emerged between 436 to 530 cm^{-1} in the complexes [17, 18]. **Table 1** displays the FTIR values. Spectra were provided in the supporting file. **Figure S3.**

Table 1

FTIR Vibrational frequencies (cm^{-1}) of Schiff base and their complexes

Compounds	$\nu_{(OH)}$	$\nu_{(C=N)}$	$\nu_{(C–O)}$	$\nu_{(M–O)}$	$\nu_{(M–N)}$
HL[1]	3453	1622	1130	-	-
A	3426	1593	1122	530	436
B	-	1609	1125	511	436
C	-	1599	1128	517	465

Electronic spectroscopy

UV – visible spectra of the ligand and its complexes A-C are provided in the **Figure S9**. The $\pi\rightarrow\pi^*$, $n\rightarrow\pi^*$ transitions of the aromatic ring (-C = C) and azomethine group (-C = N) showed their absorption bands at 257, 357 nm in the electronic spectra of the ligand which are shifted and appeared in the range 258-351 nm in the complexes **(A,B,C).** Two d-d transitions were observed in Co (II) complex, which were attributed to $^4T_1g(F) \rightarrow {}^4T_1g(P)$ and $^4T_1g(F) \rightarrow {}^4T_2g(F)$ transitions [15]. Due to $^2B_1g \rightarrow {}^2Eg$ transition Cu(II) complex displayed a single band. Ni(II) complex also showed a single band as a result of $^1A_1g \rightarrow {}^1B_1g$ transition**.** The magnetic moment values indicate that the Cu (II) and Co (II) complex, are paramagnetic and Ni(II) complexes are diamagnetic. Cu (II), Ni (II) complexes exhibits a square planar geometry and Co (II) complex exhibits an octahedral geometry, based on their electronic spectral bands and magnetic moment values.The **Table 2** lists the electronic spectral bands and magnetic moments of complexes **A**-C.

Table 2

UV-Vis spectral data (nm) and magnetic moments (BM) of A-C complexes

Compounds	n-π^*	π-π^*	CT Bands	d-d	μ_{eff} (BM)
HL[1]	257	357		-	-
A	260	351	439	555,565	4.22
B	258		425	545	-
C	259	287	415	548	1.86
Ven					

ESR spectroscopy

Figure 1 depicts the ESR spectra of Cu(II) complex recorded at -196°C in DMSO on X- band. From the results it is observed that g_{ll},> g⊥> g_e 2.0023 suggesting that the electron is localized in the dx^2-y^2 orbital, for which the ground state is the ^2B_1g with a "square planar geometry". As the g_{ll} value is smaller than 2,0023, the metal-ligand bond is covalent. According to Hathaway [19], G displays exchange interactions between M-M centers. Since G is less than four, there considerable interactions between metal centres.

The hyperfine coupling constants for complex **C** were calculated and found to be A= 0.0167 cm-1. In addition, the ratio $g_{\parallel}/A_{\parallel}$ for complex **C** was computed and found to be 131 cm, which is within the range of square planar copper(II) complexes. The observed range for the hyperfine coupling constant for square planar complexes is 105–135 cm, whereas for tetragonal deformed complexes it is > 135 cm [20].

According to the following equations, the in-plane ***σ***-bonding (α^2), in-plane ***π***-bonding (β^2), and out-of-plane ***π***-bonding (γ^2) parameters are calculated:

$$\alpha^2_{Cu} = (A_{ll}/0.036) + (gll - 2.0023) + 3/7\ (g_{\perp} - 2.0023) + 0.04$$

$$\beta^2 = (g_{ll} - 2.0023)\ E / -8\lambda\alpha_2$$

$$\gamma^2 = (g_{\perp} - 2.0023)\ E / -2\lambda\alpha_2\ ,$$

where $\lambda = 828\ cm^{-1}$ and E is the electronic transition energy. The λ value of the complex is calculated using the equation:

$$g_{av} = 1/3\ (g_{ll} + 2\ g_{\perp})\ \text{and}\ g_{av} = 2\ (1\text{-}2\ \lambda/10Dq)\ ,$$

which is foundto be 420 cm^{-1} , less than that for the free Cu (II) ion (828 cm^{-1}). This reduction in λ from the free ion value is an evidence of covalence in M–L bond [11]. The lower value of λ indicates that there is a considerable mixing of ground and excited state terms. From the calculations, it is clear that the in-plane σ-bonding parameter (α^2) is 0.719, which indicates that it has some covalent character and it is further confirmed from in-plane π-bonding β^2 value is (0.449), and out-of plane π bonding (γ^2) is 1.231. These data are well in accordance with other reported values. The following expressions are used to calculate the bonding parameters:

$$K^2_{ll} = [g_{ll} - 2.0023)\ \Delta E]\ /8\ \lambda^o$$

$$K^2_{\perp} = [g_{\perp} - 2.0023)\ \Delta E]\ /2\lambda^o\ .$$

Hathway conveyed that for pure σ-bonding, $K^2_{ll} = K^2_{\perp} = 0.77$; for in-plane π-bonding, $K^2_{ll} < K^2_{\perp}$ and for out-of-plane π-bonding, $K^2_{ll} > K^2_{\perp}$. Here, K^2_{ll} (0.323) > $K^2_{\perp}$ (0.221) which indicates the presence of out-of-plane π-bonding. μ_{eff} can also be calculated from ESR measurements using the following equation:

$$\mu_{eff} = ½(\ g_{II}^{\ 2} + 2\ g_{\perp}^{\ 2})\ ½.$$

Tvalues obtained for μ_{eff} are in accordance with observed values.

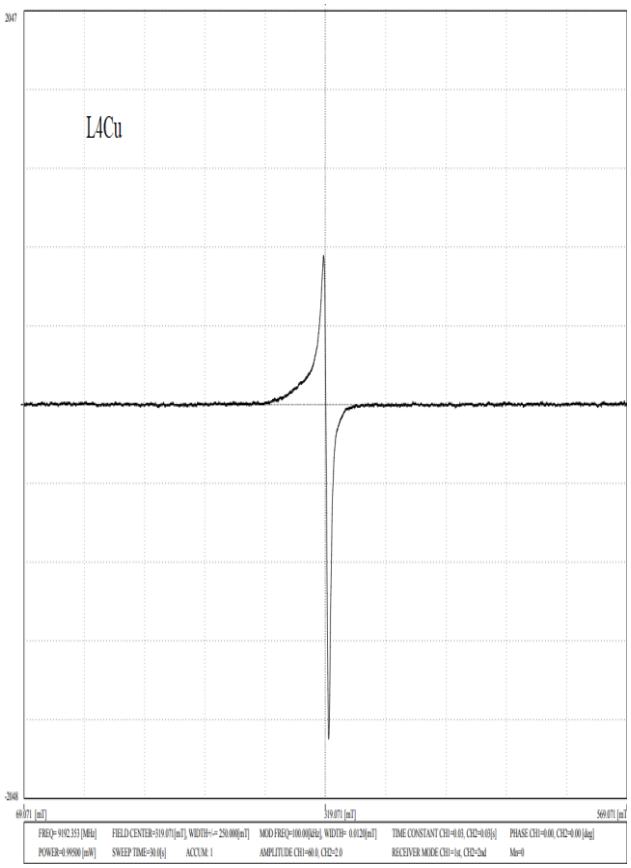

Figure 1: ESR Spectra of C Complex:

$G = (g_{ll}\text{-}2.0023) / (g_{\perp}\text{-}2.0023)$

Thermogravimetricanalysis

TGA gives the thermal decomposition of metal complexes. The TGA curves (**Figure S8)** of M (II) complexes degrade in stages. In contrast to other complexes, **complex A** begins to degrade at temperatures below 100 degrees Celsius, indicating the presence of coordinated water molecule .The loss of water and other minor moieties below 100 ^oC and the partial loss of the organic moiety between 110 and 330 ^oC in cobalt complex, with the organic moiety and metal-oxide residue remaining over 610 ^oC in cobalt complex.

Remaining complexes **B, C** are thermally stable up to 300 ^{o}C, above which degradation occurs with a partial loss of the organic moiety, and between 570 and 620 ^{o}C metal-oxide residue is remaining in nickel and copper complexes [11].

Geometrical optimization

Geometry optimized structures for complexes **A-C** were represented in **Figure 2. Table 3** lists the quantum chemical properties [21, 22] of the compounds. The selected bond angles and bond lengths obtained by chem3D application are given in **Table 4.** Molecular kinetic stability and chemical reactivity are governed by the energy difference between border molecular orbitals (highest occupied molecular orbital [HOMO] and lowest unoccupied molecular orbital [LUMO]). Various energetic statistics such as HOMO–LUMO energy gap, E_g, absolute electronegativities, χ, chemical potentials, π, absolute hardness, η, absolute softness, σ, global electrophilicity, ω, global softness, S, and additional electronic charge, ΔN_{max} were calculated. Figure S12 illustrates the HOMO and LUMO structures of compounds **A.**

Figure 2: Geometry optimized structures of complexes and ligand

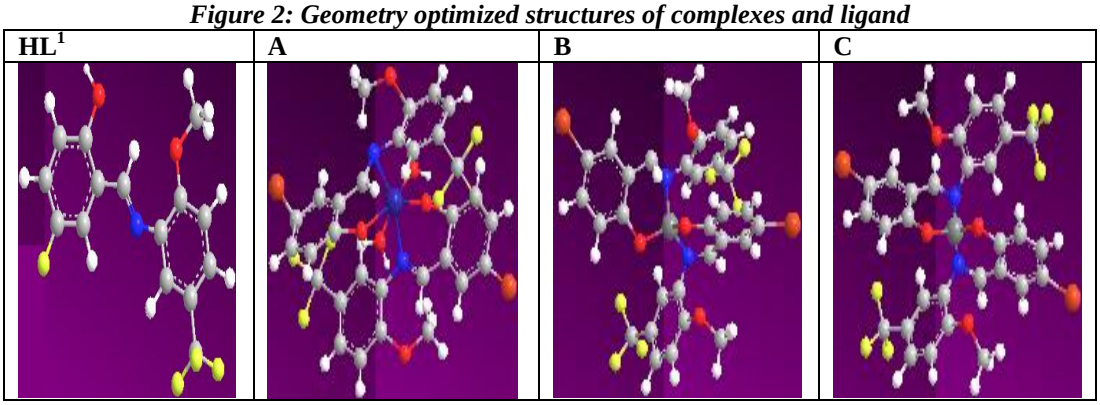

Table 3: Quantum chemical Parameters

Complex	HOMO	LUMO	Eg	χ	N	σ	π	S	Ω	ΔNmax
HL[1]	-7.281	-3.213	4.068	5.247	2.034	0.491	-5.247	0.245	6.767	2.579
A	-7.324	-3.908	3.416	5.616	1.708	0.585	-5.616	0.292	9.2328	3.288
B	-8.097	-4.56	3.537	6.328	1.768	0.565	-6.328	0.282	11.323	3.578
C	-6.341	-4.71	1.631	5.525	0.815	1.226	-5.525	0.613	18.719	6.775

Table 4: Selected bond lengths and bond angles of the complex A-C.

Complex	Atom connectivity	Bond angles	Atom connectivity	Bond lengths
A	Co(33)-O(35)	1.221	N(21)-Co(33)-O(34)	90.167
	Co(33)-O(34)	1.237	N(21)-Co(33)-O(31)	103.245
	O(31)-Co(33)	1.138	O(29)-Co(33)-N(7)	100.595
	O(29)-Co(33)	1.166	N(7)- Co(33)-O(35)	107.818
	N(21)-Co(33)	1.917	O(29)-Co(33)-O(31)	103.599
	N(7)-Co(33)	1.971	O(34)- Co(33)-O(35)	106.207
B			O(31)-Co(33)-N(7)	110.035
			O(35)-Co(33)-N(21)	118.729
			N(7)- Co(33)-O(34)	120.653
			N(21)-Co(33)-O(29)	122.265
			O(29)- Co(33)-O(35)	1258.879
			O(31)-Co(33)-O(34)	122.721
B	O(31)-Ni(33)	1.771	O(31)-Ni(33)-N(21)	104.268
	O(29)-Ni(33)	1.773	O(31)-Ni(33)-N(7)	103.837
	N(21)-Ni(33)	1.816	O(29)-Ni(33)-N(21)	105.265
	N(7)-Ni(33)	1.814	O(29)-Ni(33)-N(7)	101.501
C	O(31)-Cu(33)	1.813	O(31)-Cu(33)-N(21)	111.606
	O(29)-Cu(33)	1.813	O(31)-Cu(33)-N(7)	109.980
	N(21)-Cu(33)	1.339	O(29)-Cu(33)-N(21)	109.983
	N(7)-Cu(33)	1.339	O(29)-Cu(33)-N(7)	111.598

Kinetic studies by Coats–Redfern method

Under non-isothermal conditions, the Coats–Redfern method [23] is one of the strategies used to get thermodynamic activation parameters ((Enthalpy, Entropy, Activation energy, Gibbs free energy) for complexes **A-C.** Using TGA curves the correlation coefficients calculated from the Arrhenius plots **(Figure 3 and Table 5)** of the thermal disintegration phases fall within the range of 0.988 to 0.997, indicating a reasonable fit with a linear function. Positive G, negative S, and high activation energy levels indicate that the decomposition process is nonspontaneous and are thermally stable. The Coats–Redfern models of Complexes **(A,B,C)** are presented in the following section.

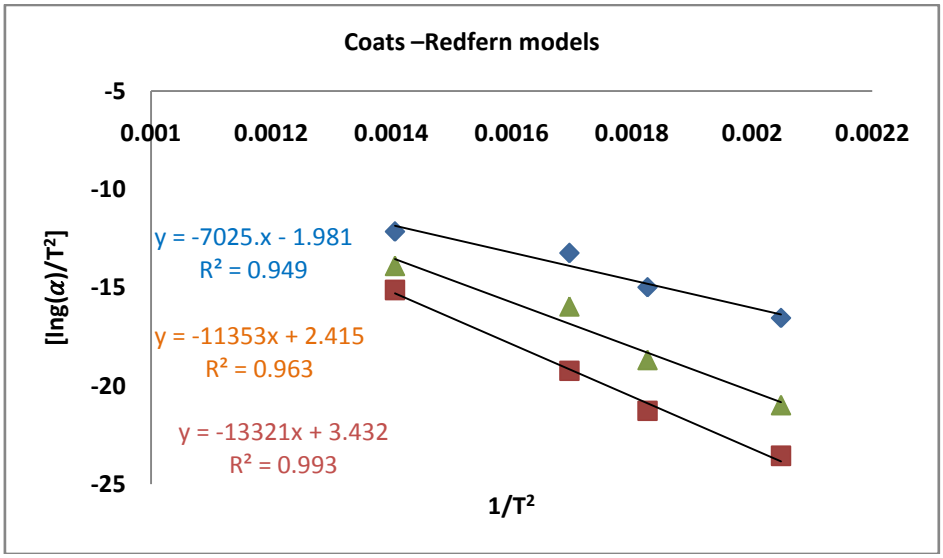

Figure 3: Coats –Redfern models of Complexes (A,B,C)

Table 5: Kinetic parameters of complexes A-C.

Complex	E_a (J mole^{-1})	ΔH(J mole^{-1})	ΔS (J mole^{-1} k^{-1})	ΔG (J mole^{-1})
A	$2.x10^4$	$4.6x10^3$	$-6.2x10^2$	$3.35x10^2$
B	$2.1x10^4$	$3.4x10^5$	$-6.5x10^5$	$4.4x10^2$
C	6.910^4	$6.5x10^3$	$-8.1x10^5$	$8.63x10^2$

The proposed structures for Metal (II) complexes are given below.

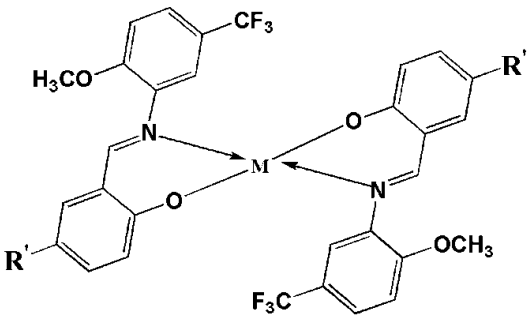

M=Ni(II), Cu(II)—B,C
R'= Br

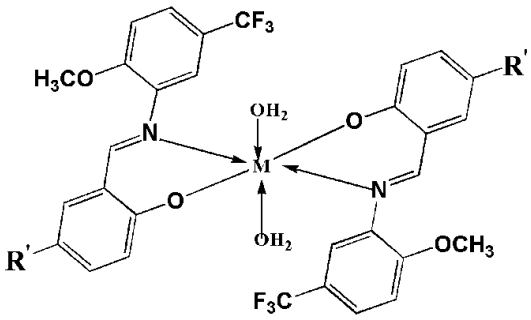

M=Co(II) --A
R'= Br

DNA binding studies:

Uv- visible absorption studies:

Using UV/Visible spectrophotometer, interactions between DNA molecules and novel compounds can be explored by observing the changes in the absorption bands, by adding gradual increasing concentrations of CT DNA. **Figure 4** depicts the impact of adding DNA while maintaining constant complex concentrations.

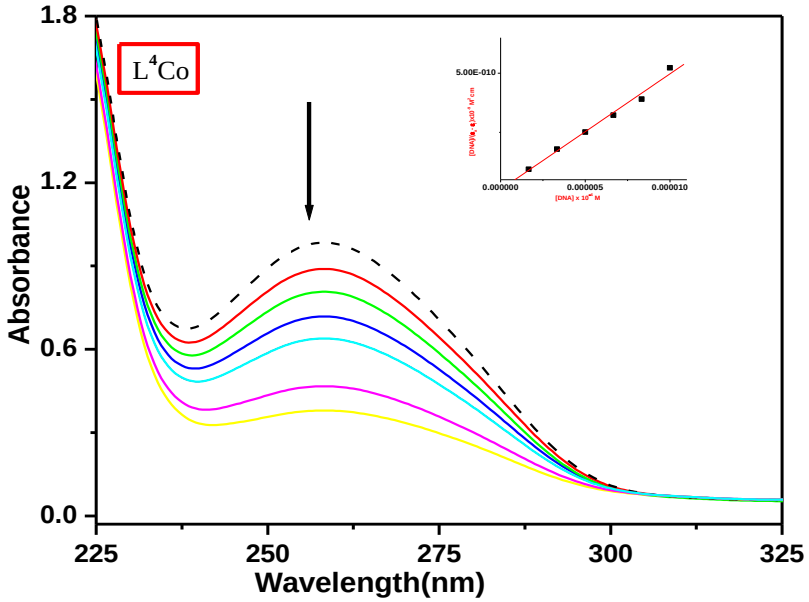

Figure 4: The UV-Vis absorption spectra of complex (A) show by dashed and solid lines, respectively, indicating the the absence and presence of CT-DNA. The arrow (↓) signifies hypochromism upon rising DNA concentrations (20, 40, 60,). Inset: a linear plot used to determine the kb values.

All spectra display hypochromism and bathochromism in the lower energy bands. The values of the binding constants for the compounds **A-C**, derived from slope by intercept values, were presented in **Table 6**. **Figure S10** depicts the remaining complexes' spectra.

Florescence studies:

EtBr-competitive experiments of M(II) complexes were also conducted using fluorescence emission spectroscopy to assess the extent of displacement of EtBr by complexes **(A-C)** from EtBr/CT- DNA system. The emission spectra of EtBr/CT-DNA were measured in the absence and presence of increasing quantities of complexes **A-C**. As the concentration of the complexes increased, the fluorescence intensity at 590 nm decreased. This strongly suggests that the complexes might replace EtBr at the intercalation site of CT-DNA. **Figure 5** depicts a representative fluorescence emission spectra of **complex A** whereas **Figure S11** displays the emission spectra of **complexes B, C.** With the addition of M(II) complexes, the fluorescence intensity of the EtBr/CT-DNA system decreases, suggesting the intercalative mode of binding of complexes **A-C** to DNA. The Stern-Volmer quenching constants (Ksv) were obtained from the slope of the plot I_0/I versus [Q], [24], and the resulting values are presented in **Table 6**.

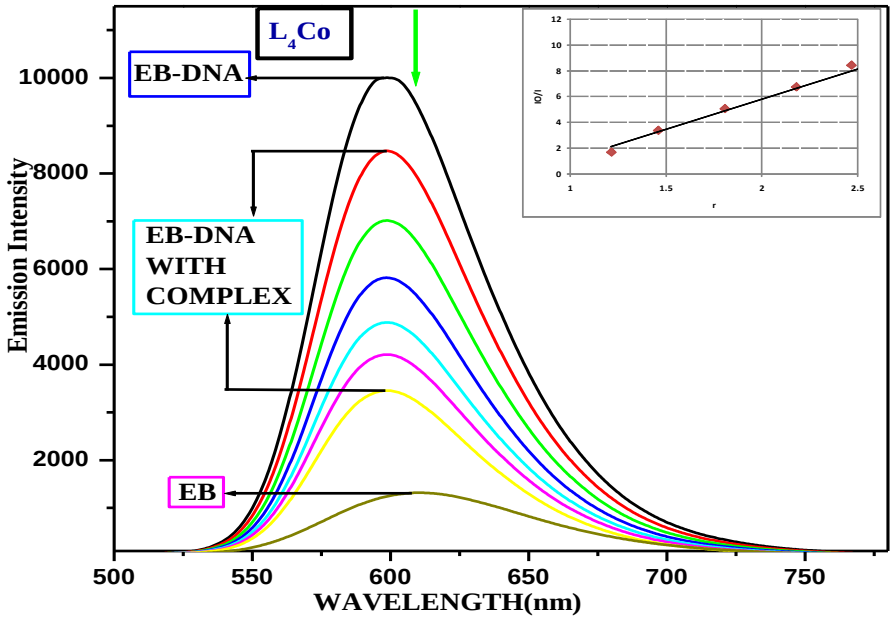

Figure 5: The dashed and solid lines show the emission spectra of EB bound to DNA in the absence and presence of complex (A). The arrow (↓) shows how the intensity changes as more of the complex concentrations (10,20,...) are added. Inset: A linear plot showing how to figure out the k_{sv} values.

Table 6: The Wolf shimmer binding constant (K_b) of the UV – visible experiment, quenching constant (K_{SV}) values of Quenching studies.

Compound	K_b	K_{sv}
A	$1.682\pm 0.02\times 10^5$	$1.312\pm 0.03\times 10^5$
B	$1.884\pm 0.03\times 10^5$	$1.753\pm 0.03\times 10^5$
C	$5.801\pm 0.02\times 10^5$	$5.532\pm 0.03\times 10^5$

Cleavage studies

Agarose Gel electrophoresis

In order to understand DNA cleavage by the compounds under study, both photolytic and oxidative cleavage experiments were performed by gel electrophoresis method and represented in figures **6.1 , 6.2.** The pBR 322(2 **µ**M) and the compounds (10 **µ**M) were incubated for one hour at 37 degrees Celsius in a medium 5 mM TrisHCl/50 mM NaCl solution containing bromo phenol blue as a tracking dye. The supercoiled form will display the fastest migration when the reaction mixture is subjected to electrophoresis (SC, Form I). If one strand is broken, the supercoiled form will relax into a nicked, slow-moving form (NC, Form II). If both strands are cleaved, a linear form (LC, Form III) that migrates between SC and NC forms will result. In the initial step, we propose reducing the complex M(II) with peroxide to form the M(I) species. M(I) reacts with O_2 to generate superoxide anion (O_2•) followed by H_2O_2. The M(I) produced and bonded to DNA to form the (DNA)-M(I) adduct, which reacts with hydrogen peroxide to form a free hydroxide ion and a DNA-bound M(II)-hydroxyl radical intermediate [25]. This creates a radical focused on deoxyribose [26].In photolytic cleavage mediated by compounds indicates the involvement of singlet oxygen ($^1O_2$) as the reactive species. As suggested by Toshima et al [27] the triplet states resulting from the n–p*and p–p* photo-excitation in the UV radiation could activate oxygen to form $^1O_2$ that cleaves DNA . In both photolytic and oxidative cleavage, all complexes were cleaved into Form-II.

Oxidative cleavage of ligand and complexes A-C:

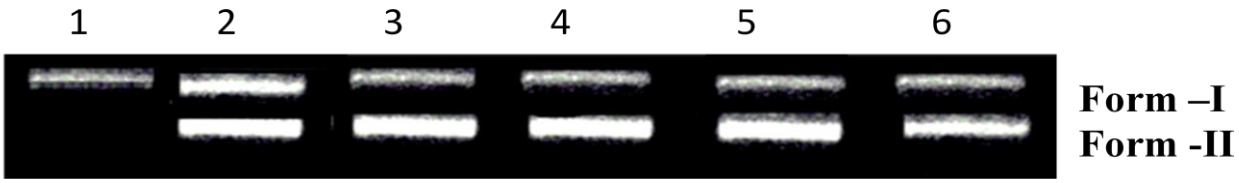

Figure 6.1: The complexes triggered cleavage of supercoiled pBR322 DNA (0.2µ g, 33.3 µM) at 37 °C in 5mM Tris HCl/5 mM NaCl buffer by the peroxide. Lane **1**-DNA control, Lane **2**-DNA+H_2O_2, **Lane 3-6** (DNA+ **ligand HL[1] and complexes A-C).**

Photolytic cleavage of ligands and complexes A-C:

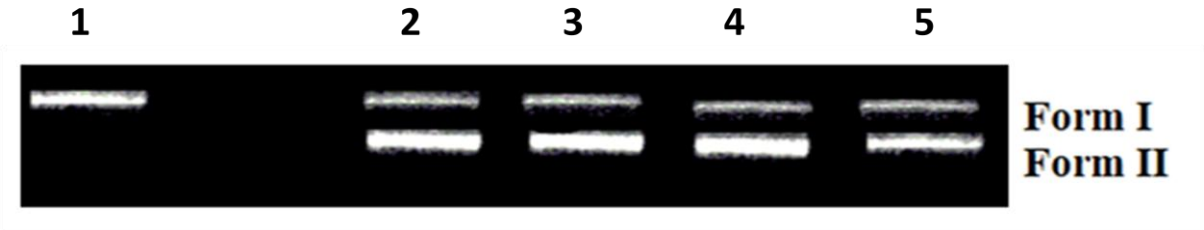

Figure 6.2: The complexes triggered cleavage of supercoiled pBR322 DNA (0.2µ g, 33.3 µM) at 37 °C in 5mM Tris HCl/5 mM NaCl buffer (long UV-365 nm) in the UV-light (long UV-365 nm). **Lane 1**-DNA control, **Lane 2-5** (DNA+ **HL[1]**, **complexes A-C**).

Biological Activity

α-glucosidase inhibitory activity

α-glucosidase inhibitory activity [28] was performed to know the antidiabetic activity of the complexes**. Table 8** represents the IC_{50} values of the compounds. In which the copper complex exhibited more activity than other complexes and also the standard acarbose. **Table** 7 also showed that, compared to other complexes copper complex exhibited a stronger effect on the a-glucosidase enzyme. Complex C were the most active with an IC_{50} value of 0.01, which is higher than the standard drug.

Table 7 : α-glucosidase inhibitory activity of test compounds in their IC_{50} values :

Compounds	IC_{50} (µM)
A	14.5±2.9
B	21±2.5
C	0.01
Acarbose	0.08

Radical scavenging activity

The ability of a chemical to transfer a hydrogen atom (HAT) is one of the determinants of its DPPH-scavenging activity [29]. By using DPPH radical scavenging method the antioxidant property was performed. The calculated half minimum inhibitory concentration (IC_{50}) values for complexes **A-C** are presented in the **Table 8** below. The influence of complexes and standards on the radical scavenging capacity of the DPPH radical increases in the order **B<A<C<AA. Figure 7**. Cu(II) Complex showed stronger radical scavenging effects than other complexes on DPPH techniques with lower IC_{50} values, but less activity than ascorbic acid.

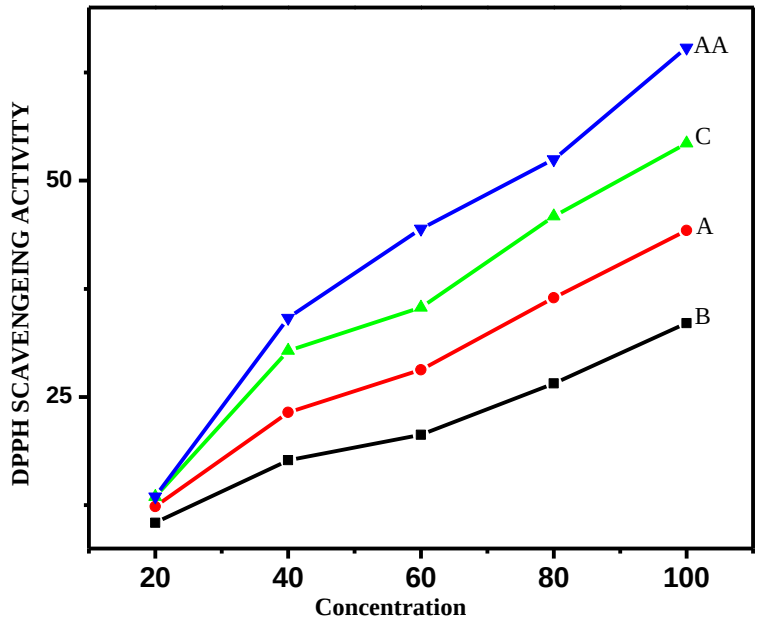

Figure 7: Anti oxidant properties of the complexes A-C

Table 8: IC_{50} values the complexes in DPPH activity:

Compounds	IC_{50} values
A	40±0.18
B	35±0.02
C	22±0.02
AA	18±0.12

Anti microbial assay

The antimicrobial activity of the ligand and its metal complexes with Co(II), Ni(II), and Cu(II) was evaluated against (i) Gram-positive bacteria, such as B. cereus and Bacillus subtilis, (ii) Gram-negative bacteria, such as Escherichia coli, K. Pneumoniae and (iii) fungal strains, such as A.niger, C.albicans. The inhibition zones are depicted graphically in **Figure 8**. The zone of inhibition values are given in the **Table** 9. From the results it is found that the metal complexes are effective against bacteria and fungi, than corresponding ligand .The order of the activity is found to be Cu (II) > Co(II) > Ni(II). The enhanced activity of the complexes can be explained using Overtone's concept [30] and Tweedy's Chelation theory [31].

Table 9: The zone of inhibitions of the compounds.

	B. subtilis	***E. coli***	***K. Pneumoniae***	***B. cereus***	***A.niger***	***C.albicans***
HL^1	9	10.2	7.1	8.6	4.4	5
A	24.5	20.6	21.5	23.1	6.2	4.4
B	8.4	7.7	8.7	9.1	2.5	2.5
C	24.8	24	21.8	22.8	6.5	5.5
Gentamicin sulphate	29.1	32.6	29.3	31	-	-
Nystatin	-	-	-	-	29.8	26.1

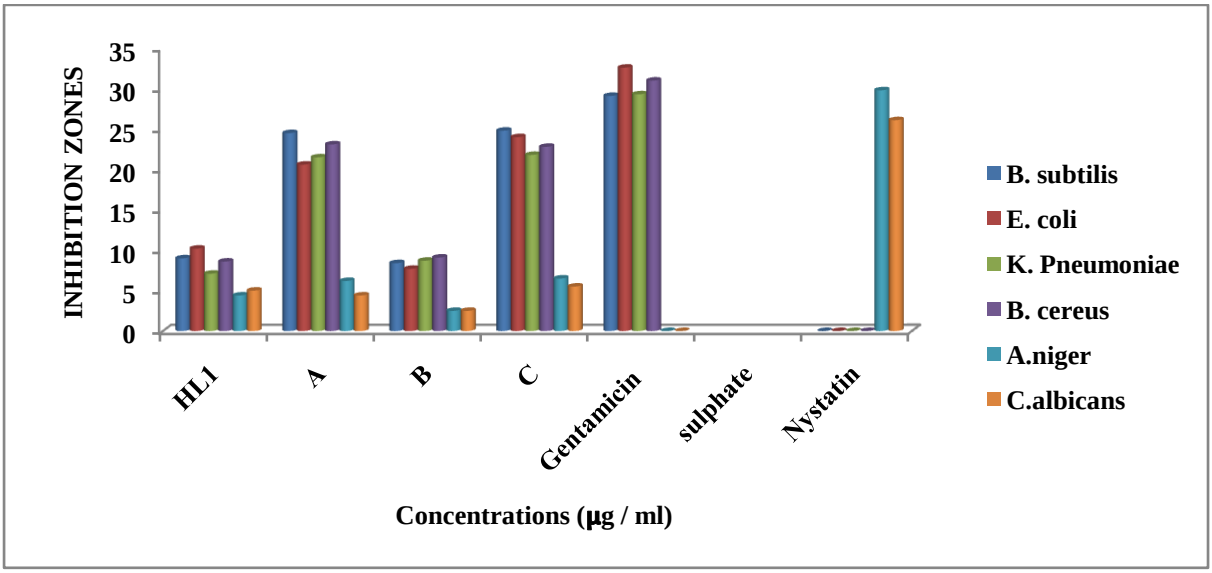

Figure 8: Antimicrobial data of parent ligand and its metal (II) complexes (A-C) at 500 go/mL concentration

Cytotoxicity

The in vitro antiproliferative activity of ligand and its respective complexes were evaluated using a range of MCF7 and KB3 human cancer cell lines. **Figure 9.a and 9.b** demonstrate that these compounds impede the development of these cancer cells. It is found that the metal complexes were more cytotoxic than the Schiff base. The results of the ligand capacity to bind and cleave DNA are consistent with the observation that metal complexes can demonstrate more pharmacological action than free ligand [32]. Comparing the cytotoxicity of the complex to the cytotoxicity of the free ligand demonstrates that the incorporation of metal into the ligand moiety has a significant effect on the antiproliferative activity. Coordination decreases the polarity of the ligand and the central metal ion via charge equilibration, hence promoting the penetration of complexes across the lipid layer of the cell membrane [33, 34]. Comparing the percentage of alive cells, all the complexes demonstrate good cytotoxicity, as indicated by their IC_{50} values **(Table 10),** which are consistent with the DNA binding findings.

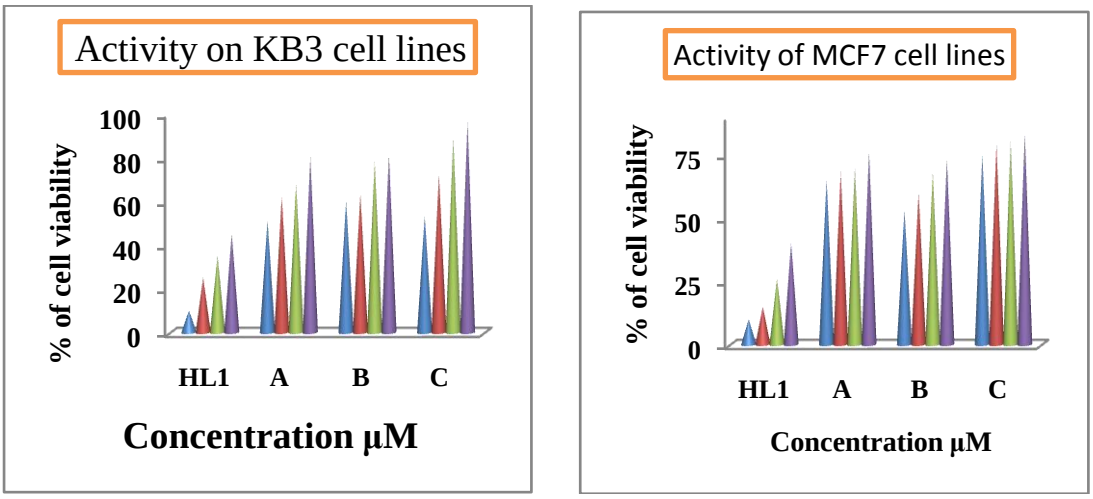

Figure 9Anticancer activity of KB3 and MCF7cell lines

Table 10: IC_{50} values (µM) of the compounds

Compounds	MCF7	KB3
HL[1]	16±0.41	18±0.21
A	18±0.51	19±0.81
B	19.2±0.35	18.3±0.42
C	10.2±0.15	11.5±0.23
Cis Platin	<2.27	<2.52

IV. Conclusion

New Schiff base HL^1 was used to design three bio**e**fficient **(A–C)** complexes. Spectroanalytical methods were used to figure out their structure and bonding. The Ni(II) and Cu(II) complexes exhubited a square planar geometry, while the Co(II) complex exhibited an octahedral geometry. These were further confirmed by geometrical optimization. The TGA experimenta resulted that these complexes are thermally stable. With the help of the Coats-Redfern method, the kinetic parameters have been evaluated. The DNA interaction techniques showed that the complexes bind to CT-DNA in an intercalative mode, and the Cu(II) complex bind more strongly than other complexes (**C > B > A)**. DNA cleavage tests showed that both photolytic and oxidative cleavage studies revealed that the complexes and ligand have been able to incise supercoiled pBR322 DNA into Form II. Alpha-glucosidase inhibitory activity showed that copper complex exhibited more activity than standard (Acarbose). The complexes are better at getting rid of free radicals than ligand, but not as good as the standard drug (ascorbic acid). The biological tests showed that the complexes were more effective than the free Schiff base against bacterial and fungal strains. Further, the results showed that Cu(II) complexes are more potent than other compounds. Experiments on cell viability showed that the ligand and its compiexes are potent anticancer effect against KB3 and MCF-7 cell lines. Further it is observed that copper complex **C** exhibited more activity than Co(II) and Ni (II) complexes.

References

[1]. Liu H-K, Sadler PJ. Metal Complexes as DNA Intercalators. Acc. Chem. Res. 2011;44(5): 349-359.

[2]. Simunkova M, Lauro P, Jomova K, Hudecova L, Danko M, Alwasel S, Alhazza IM, Rajcaniova S, Kozovska Z, Kucerova L, Moncol J, Svorc L, Valko M. Redox-cycling and intercalating properties of novel mixed copper(II) complexes with non-steroidal anti- inflammatory drugs tolfenamic, mefenamic and flufenamic acids and phenanthroline functionality: Structure, SOD-mimetic activity, interaction with albumin, DNA damage study and anticancer activity J. Inorg. Biochem. 2019;194: 97-113.

[3]. A. M. Abu-Dief, L. H. Abdel-Rahman, M. R. Shehata, A. A. H. Abdel-Mawgoud. Novel azomethine Pd (II)- and VO (II)-based metallo-pharmaceuticals as anticancer, antimicrobial, and antioxidant agents: Design, structural inspection, DFT investigation, and DNA interaction. J. Phy. Org. Chem. 2019;32(12): e4009

[4]. Salehi, M.; Faghani, F.; Kubicki, M.; Bayat, M. New complexes of Ni(II) and Cu(II) with tridentate ONO Schiff base ligand: synthesis, crystal structures, electrochemical and theoretical investigation. J. Iran. Chem. Soc. **2018**;15:2229– 2240.

[5]. Cozzi PG, Metal-salen Schiff base complexes in catalysis: practical aspects, Chem. Soc. Rev. 2004;33:410–421.

[6]. Gupta KC, Sutar AK. Catalytic activities of Schiff base transition metal complexes. Coord. Chem. Rev. 2008;252:1420–1450.

[7]. Kenneth DK, Itoh S, Rokita S. Copper-Oxygen Chemistry. John Wiley & Sons, United Kingdom, 2010.

[8]. Manikandamathavan VM, Rajapandian V, Freddy V, Weyhermuller T, Subramanian V, Nair BU. Effect of coordinated ligands on antiproliferative activity and DNA cleavage property of three mononuclear Cu(II)-terpyridine complexes. Eur. J. Med. Chem. 2012;57: 449-458.

[9]. E.R. Jamieson, S.J. Lippard. Structure, Recognition, and Processing of Cisplatin−DNA Adducts, Chem. Rev., 1999;99: 2467-2498.

[10]. K.E. Erkkila, D.T. Odom, J.K. Barton. **Recognition and Reaction of Metallointercalators with DNA** Chem. Rev. 1999; 99(9):2777-2789.

[11]. Venkateshwarlu K., Anantha Lakshmi, PV, Shivaraj, Synthesis, spectroscopy and thermal studies of Cu^{+2},Ni^{+2} and Co^{+2} of Schiff base containing furan moiety.Anti tumor, anti oxidant, anti microbial and DNA interaction studies. Appl organomet chem. 2022; 36 :6530.

[12]. Daravath, S Rambabu, A, Ganji, N, Ramesh, G, Anantha Lakshmi PV, Shivaraj, Spectroscopic, quantum chemical caliculations, antioxidant, anticancer, antimicrobial, DNA binding and photophysical properties of bioactive Cu(II) complexes obtained from trifluoromethoxy aniline Schiff bases, J. Mol. Str. 2022;1249:131601

[13]. Shankar DS, Ganji, N, Daravath, S, Venkateswarlu, K., Shivaraj, Evaluation of DNA interaction,free radical scavenging and biologically active compounds ofthermally stable p-tolylmethanamine Schiff bases and their binary Co(II) Ni(II) Cu(II) metal complexes, Chem. Data Collect.2020;28:100439.

[14]. Rambabu A, Daravath, S, , Shankar DS Shivaraj, DNA-binding-cleavage and anti- microbial investigation on mononuclear Cu(II) Schiff base complexes originated from Riluzole, J. Mol. Struct 2021;1244 :13100.

[15]. Venkateswarlu K, Rambabu A, Shankar DS Daravath S,.Anantha Lakshmi, PV, Shivaraj, A Treatise on Furan Cored Schiff Base Cu(II), Ni(II) and Co(III) Complexes Accentuating Their Biological Efficacy: Synthesis, Thermal and Spectroscopic characterization, DNA Interactions, Antioxidant and Antibacterial Activity Studies, Chem. Biodiversity. 2022;19: e202100686.

[16]. Jyothi, N. Ganji N, Daravath, S. Shivaraj, Mononuclear cobalt(II), nickel(II) and copper(II) complexes: Synthesis, spectral characterization and interaction study with nucleotide by in vitro biochemical analysis, J. Mol. Struct. 2020;1207:127799.

[17]. Venkateswarlu K, Kumar MP, Rambabu A, Vamsikrishna N, Daravath S, Rangan K, Shivaraj, Crystal structure, DNA binding, cleavage, antioxidant and antibacterial studies of Cu(II), Ni(II) and Co(III) complexes with 2-((furan-2-yl)methylimino)methyl)-6-ethoxyphenol Schiff base, J. Mol. Struct. 2018, 1160:198–207.https://doi.org/10.1016/j.molstruc.2018.02.004.

[18]. zhou Y, Liu L, Yang M, Lu R, Jin Y, Chen W, Synthesis, crystal structure and biological property of a novel phenolato-bridged trinuclear copper(II) complex derived from bis-Schiff base ligand. Inorg. Nano-Met. Chem. 2019; 48, 291-295.

[19]. Hathaway BJ, Billing DE, The electronic properties and stereochemistry of mono-nuclear complexes of the copper(II) ion, Coord.Chem. Rev. 1970;5:143.

[20]. Nickless DE, Power MJ, Urbach FL, Copper(II) complexes with tetradentatebis(pyridyl)-dithioether and bis(pyridyl)-diamine ligands. Effect of thio ether donors on the electronic absorption spectra, redox behavior, and EPR parameters of copper(II) complexes**,** Inorg. Chem. 1983;22:3210-3217.

[21]. Obot I, Obi N, HSAB descriptors of thiadiazole derivatives calculated by DFT: possible relationship as mild steel corrosion inhibitors, Der PharmaChemica. 2009;1: 106-123.

[22]. Navaneetha N, Ramasree D. Kumar MK, Vasavi M, Nagababu VUP, Satyanarayana S, Molecular dynamic simulations of Co(III)and Ru(II) polypyridyl complexes and docking studies with dsDNA, Med Chem Res. 2013;22:5557-5565.

[23]. Vasantha p, Vasantha P, Kumar BS, Shekhar B, Anantha Lakshmi PV, Copper-metformin ternary complexes: Thermal, photochemosensitivity and molecular docking studies .Mater.Sci. Eng. C. 2018; 90: 621.

[24]. Chen J, X. Wang X, Shao Y, Zhu J, Zhu Y. Li Y, Xu Q, Guo Z, A trinuclear copper(II) complex of 2,4,6-Tris(di-2-pyridylamine)-1,3,5-triazine shows prominent DNA cleavag e activity, Inorg. Chem. 2007;46:3306–3312.
[25]. Kuwabara MD, Yoon C, Goyne T, Thederahn T, Sigman DS, Nuclease activity of 1,10-phenanthroline-copper ion: reaction with CGCGAATTCGCG and its complexes with netropsin and EcoRI, Biochemistry.1986,25:7401–7408.
[26]. Sigman DS, Kuwabara MD, Chen CB, Bruice TW, Nuclease activity of 1,10- phenanthroline-copper in study of protein-DNA interaction, Methods Enzymol. 1991;208: 414–433.
[27]. Toshima K., Takano R, Ozawa T. and Matsumura S., Molecular design and evaluation of quinoxaline-carbohydrate hybrids as novel and efficient photo-induced GG-selective DNA cleaving agents Chem. Commun. (2002) 212.
[28]. Clissold SP, Edwards C, Acorbose a preliminary review of its pharmacodynamic and pharmacokinetic properties, and therapeutic potential. Drugs. 1998;35(3) :214-243.
[29]. Wright JS, Johnson ER Di Labio GA, Predicting the activity of phenolic antioxidants: theoretical method, analysis of substituent effects, and application to major families of antioxidants, J. Am. Chem. Soc. 2001;123(6):1173–1183.
[30]. Parekh J, Inamdhar P, Nair R, Baluja S. Chanda S**,** Synthesis and antibacterial activity of some Schiff bases derived from 4-amino benzoic acid J. Serb. Chem. Soc. 2005; 70: 1161.
[31]. Tweedy BG, Plant extracts with metal ions as potential antimicrobial agents Phytopathology 1964;55:910
[32]. Rosu T, Pahontu E, Pasculescu S, Georgescu R, Stanica N, Curaj A, Popescu A, Leabu M, Synthesis, Characterization antibacterial and antiproliferative activity of novel Cu(II) and Pd(II) complexes with 2-hydroxy-8-R-tricyclotridecane-13-one thiosemicarbazone Eur. J. Med. Chem. 2010;45:1627–1634
[33]. Ramadan AM, Structural and biological aspects of copper (II) complexes with 2-methyl-3-amino-(3 *H*)-quinazolin-4-one, J. Inorg. Biochem. 1997; 65:183–189.
[34]. Avaji PG, Kumar CHV, Patil SA, Shivananda KN, Nagaraju C, Synthesis, spectral characterization, in-vitro microbiological evaluation and cytotoxic activities of novel macro cyclic bis hydrazone. Eur. J. Med. Chem. 2009; 44:3552–3559.

Shivaraj. et. al. "DNA Interactions, Biological activities of Co(II), Ni(II), Cu(II) Complexes of 2-methoxy 5-trifluoromethyl benzenamine Schiff base: Synthesis, Characterization." *IOSR Journal of Applied Chemistry (IOSR-JAC),* 16(2), (2023): pp 64-77.